



A Study of Electromagnetic Vibration Energy Harvesters: Design Optimization and Experimental Validation

Seok-Chan Kim¹ · Jin-Gyun Kim² · Young-Cheol Kim³ · Seok-Jo Yang¹ · Hanmin Lee³

Received: 17 December 2018 / Revised: 17 June 2019 / Accepted: 23 June 2019 / Published online: 19 July 2019
© Korean Society for Precision Engineering 2019

Abstract

The aim of this study is to optimize the electromagnetic vibration energy harvesters with typical cylindrical shape considering the aspect ratio. In the optimization procedure, voltage and power, which are two key factors of energy harvesting systems, are mainly considered in the three types of electromagnetic vibration energy harvester according to various aspect ratios. We then investigate the optimum design parameters in each case. The results show that there is an optimum aspect ratio that maximizes the output voltage and power for the same volume. We also find that the optimum design parameters for each aspect ratio have a relatively constant value regardless of the aspect ratio. An experimental study is also conducted to verify the simulation results of the design optimization, and it clearly confirms that the proposed optimization result matches the experimental results well.

Keywords Electromagnetic energy harvester · Design optimization · Aspect ratio · Transduction factor

1 Introduction

Nowadays, the Internet of Things and wireless sensor networks are essential in various engineering fields, such as electric vehicles, implantable medical devices, and cyber-physical systems. However, the problem of how to supply electric power to wireless sensor nodes remains a major obstacle. To solve this problem, various studies on energy harvesting, which makes electrical energy from ambient energy, have been conducted recently.

The vibration energy harvester is a device that converts kinetic energy such as vibration (or shock) into electric energy. It can be divided into piezoelectric, electromagnetic,

and electrostatic types depending on the energy conversion method. The electromagnetic vibration energy harvester uses Faraday's law in which the electromotive force is induced by the relative movement between the magnet and the coil, and it has a great advantage in terms of the output density and design flexibility in comparison with other methods [1].

Much research has been done on the vibration energy harvester to date [2–9]. Recent studies have focused on design optimization to maximize the productivity of the electromagnetic vibration energy harvester. Spreemann et al. [10, 11] classified the type of harvester into seven types according to the direction of the axis of the moving magnet and the presence of an iron core and obtain the optimal design parameters for the output voltage and power. Cepnik et al. [12, 13] performed nonlinear magnetic field analysis and proposed a design guideline of the harvester for the maximum output power. However, these studies have not examined the output characteristics according to the aspect ratio, which is a main factor in determining the shape of the energy harvester. Hence, Kim et al. [14] studied preliminary design optimization for the electromagnetic vibration energy harvester according to the aspect ratio, but the results were not verified in an experimental way.

To overcome this problem, we here carefully designed three types of electromagnetic vibration energy harvester considering various aspect ratios; this study can be carried out by

✉ Hanmin Lee
hmlee@kimm.re.kr

¹ Department of Mechatronics Engineering, Chungnam National University, 79, Daehak-Ro, Yuseong-gu, Daejeon 34134, Republic of Korea

² Department of Mechanical Engineering, Kyung Hee University, 1732, Deogyong-daero, Giheung-gu, Yongin-si, Gyeonggi-do 17104, Republic of Korea

³ Department of Smart Industrial Machine Technologies, Korea Institute of Machinery and Materials, 156, Gajeongbuk-Ro, Yuseong-gu, Daejeon 34103, Republic of Korea

experimental verification. In the design optimization, we computed the output voltage and power according to the aspect ratio of each type and analyzed the optimum design parameters for each type and aspect ratio. The output voltage and power were efficiently computed by combining the numerical and analytical approaches, that is, the magneto-static finite element (FE) analysis and the ordinary differential equation of electromagnetic vibration. In the design optimization process, to consider nonlinearity, we made an approximate optimal design using a 9-level orthogonal array and kriging method. In the experimental analysis, the output power for the energy harvester types suggested in this paper was measured considering the aspect ratio, and the experimental result verified the optimal aspect ratio for each type of harvester and validated the FE model. To obtain the generalization result of design optimization, we defined the design parameters as a dimensionless ratio so that the result of this study can be applied regardless of the size of the harvester. Our study will provide a guideline on the design of the electromagnetic vibration energy harvester.

In the following sections, we first explain the systems of the electromagnetic vibration energy harvester and the process of calculating the transduction factor using FE analysis in Sect. 2. Section 3 presents the theoretical background of the optimization process used in this work. In Sect. 4, we present the experimental validation and methods, and conclusions are given in Sect. 5.

2 Theoretical Background

2.1 Power Equation of Mechanical-to-Electrical Conversion

In this section, we briefly introduce the governing equations of a typical electromagnetic energy harvester (EMEH), which is described in Fig. 1. It can be expressed by the following differential equations:

$$m\ddot{z}(t) + c\dot{z}(t) + kz(t) = -m\ddot{y}(t), \quad (1)$$

$$L_c \frac{d}{dt} i(t) + (R_{coil} + R_{load}) i(t) = k_t \dot{z}(t), \quad (2)$$

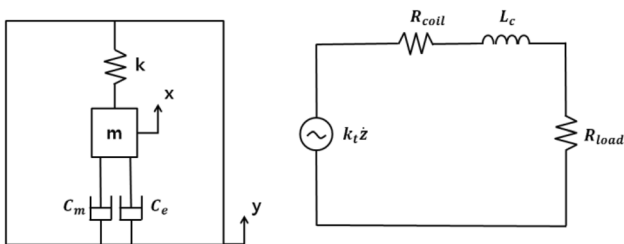


Fig. 1 Electromagnetic vibration energy harvester mechanical system (left) and electrical system (right)

where m , c and k denote the mass, damping and spring constant, respectively. The damping constant c can be defined by the sum of the mechanical and electrical damping constants, which are denoted by c_m and c_e , respectively. $x(t)$ and $y(t)$ are the absolute displacements of the magnet and housing, respectively, and $z(t)$ means those relative displacements. L_c , k_t , R_{coil} and R_{load} are the coil inductance, transduction factor, coil resistance and load resistance, respectively. $i(t)$ is the current flowing through the coil, and the time variable is denoted by t . The mechanical and electrical damping constants, c_m and c_e , in Eq. (1) are then defined by:

$$c_m = 2m\omega_n\zeta_m, \quad \omega_n = 2\pi f_n, \quad (3)$$

$$c_e = \frac{k_t^2}{R_{coil} + R_{load}}, \quad (4)$$

which ω_n and ζ_m are the natural frequency and mechanical damping coefficient, respectively

Assuming the harmonic excitation $y(t) = Y \sin \omega t$, the steady state solution of Eq. (1) is then obtained as:

$$z(t) = A_1 \sin \omega t + A_2 \cos \omega t, \quad (5)$$

$$A_1 = \frac{mY\omega^2(c\omega)}{(k - m\omega^2)^2 + (c\omega)^2}, \quad A_2 = \frac{mY\omega^2(k - m\omega^2)}{(k - m\omega^2)^2 + (c\omega)^2}. \quad (6)$$

It can also be rewritten as:

$$z(t) = Z \sin(\omega t + \varphi), \quad (7)$$

$$Z = \frac{mY\omega^2}{\sqrt{(k - m\omega^2)^2 + (c\omega)^2}}, \quad (8)$$

$$\varphi = \frac{A_1}{A_2} = \frac{c\omega}{k - m\omega^2}. \quad (9)$$

In a similar way, we can also compute \dot{Z} as:

$$\dot{Z} = \frac{mY\omega^3}{\sqrt{(k - m\omega^2)^2 + (c\omega)^2}}. \quad (10)$$

In a small energy harvester, the effect of the coil inductance L_c can be ignored, and thus we define $i(t)$ from Eq. (2) as:

$$i(t) = \frac{k_t \dot{z}(t)}{R_{coil} + R_{load}}. \quad (11)$$

From the study by Stephen[15], the optimum load resistance $R_{load,opt}$ that maximizes the output power is calculated from Eq. (12) as:

$$R_{load,opt} = R_{coil} + \frac{k_t^2}{c_m}. \quad (12)$$

Table 1 Vibration conditions

Description	Symbol	Value
Magnitude of acceleration	Y	2.5 m/s
Vibration frequency	f	100 Hz
Mechanical damping ratio	ζ_m	0.01

According to Eqs. (10) and (11), the maximum output voltage of the harmonic excitation is given by:

$$V_{\max} = \frac{R_{\text{load}}}{(R_{\text{coil}} + R_{\text{load}})} k_t \dot{z}. \tag{13}$$

In this study, the effective value of the maximum voltage from the load resistance V_{rms} is expressed by:

$$V_{\text{rms}} = \frac{V_{\max}}{\sqrt{2}}, \tag{14}$$

and the output power P_{avg} is expressed using Ohm’s law as

$$P_{\text{avg}} = \frac{V_{\text{rms}}^2}{R_{\text{load}}}. \tag{15}$$

We here assumed the external excitation as a sine wave form with the vibration conditions described in Table 1, which are based on Spreemann and Manoli [1]. The output power and voltage were then computed from Eqs. (1) and (2) using Matlab.

2.2 Electromechanical Transduction Factor by Using Maxwell’s Theory

In this work, we considered the typical cylindrical shapes of the electromagnetic vibration energy harvester [1], which coincides with the direction of relative movement of the rotating axis of the coil and the magnet. In this case, the area of the coil is fixed, while the magnetic flux density crossing the coil changes with time. Therefore, to calculate the transduction factor, it is necessary to additionally calculate the rate of change of the magnetic flux density along the distance, so that the calculation is complicated and error is liable to occur [16].

To solve this problem, the rate of change in the magnetic flux density along the distance is expressed by the Gauss magnetic law with respect to the B_ρ magnetic flux density in the radial direction with the relative movement between the magnet and the coil as:

$$\frac{dB}{dz} A \cong -B_\rho l, \tag{16}$$

where A denotes the area of the coil that intersects the magnetic flux. The transduction factor k_t is then expressed as:

$$k_t = -NB_\rho l. \tag{17}$$

The transduction factor can be calculated only by the magnetic flux density in the radial direction without calculating the rate of change of the magnetic flux density with the distance [15]. In this case, the total number of turns of the coil N is expressed in the form of a design variable [15] as:

$$N = \frac{4k_{co}(R_o - R_i)h_{coil}}{\pi d_{co}^2}, \tag{18}$$

in which, k_{co} is the filling factor of the coil, and d_{co} is the diameter of the coil.

The magnetic flux density in the radial direction can be calculated by finite element analysis. The mesh size of the magnets, coils, and air gap are 0.5, 0.2 and 0.5 mm, respectively. In this work, ANSYS Maxwell software was used to compute the electromechanical transduction factor. Generally, it is necessary to integrate the magnetic flux density in the radial direction distributed over the entire coil area.

However, considering the efficiency of the calculation, the transduction factor was calculated using a method in which the coil area is divided vertically and averaged the transduction factor calculated for each cell [17]. The cross section of the coil can be divided into the n ’th line as shown in Fig. 2, and the magnetic flux density in the radial direction distributed on the vertical line passing through the center of each cell can be calculated. The transduction factor was then computed as:

$$k_t = N \frac{\sum_{k=1}^n 2\pi R_k B_k}{n}, \tag{19}$$

where R_k is the radial distance to the center of the k th cell. B_k is the averaged value of the magnetic flux density in the radial direction for each cell. In this study, the cross section of the coil was divided into seven sections considering the convergence and calculation efficiency.

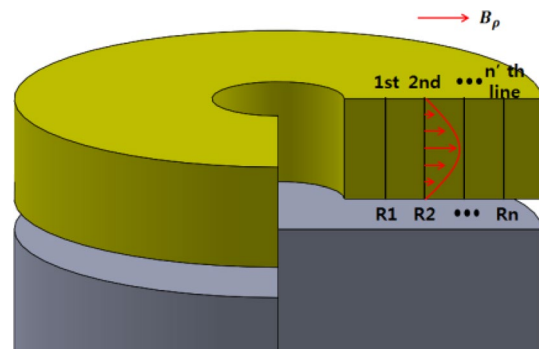


Fig. 2 The cross section of the coil divided in to n ’th line

2.3 Design of Experiment and Approximate Model

The design optimization procedure suggested in this study has the following steps. First, we select the harvester type and the sampling design parameters using the design of experiment (DOE) method. In the next step, we calculate the output voltage and power from the numerical integration of the system's differential equation and the transduction factor, which are computed by finite element analysis. Finally, we create an approximate model (metamodel) based on the output result for each sample and the optimum design is derived from the approximate model.

The process of the design optimization can be roughly divided into two steps, the DOE and the metamodel. The design of computer experiments fills the design space equally and there are various methods for this. The orthogonal array suggested by Owen [18], is used in the DOE method, which distributes the design parameters throughout the design space with a high sampling level.

In the metamodeling process, the selection of an approximate model is an important factor in accurately predicting the result of design optimization. There are many metamodeling approaches known to date. Among them, in this study, we selected the kriging method, which can represent the nonlinearity of the output performance for the harvester, as an approximate model. The kriging model is expressed by the following equation:

$$y(x) = f(x) + Z(x), \quad (20)$$

where $f(x)$ denotes the global model in the design domain, which can be expressed as a linear or polynomial function about design parameter x . $Z(x)$ is a function that expresses in a probabilistic model the local deviation between a sampling point and the global model, and $y(x)$ denotes the kriging approximation function. The optimum design is derived from the result of $y(x)$, which is obtained by considering the design parameters for each type.

3 Optimization Result Based on Analytical Methods

3.1 Model Definition

In this study, we consider the typical type of electromagnetic vibration energy harvester [1]. Then, the magnet, the coil, and the housing are assumed as having a cylindrical shape, and the structure in which the direction of rotation of the coil and the direction of movement of the magnet coincide with each other. The detailed design of the three types of harvester is shown in Fig. 3.

Type 1 is a structure in which one end of a magnet enters inside a coil. The design parameters we used for optimization of Type 1 are the ratio of the radius of the entire volume to the radius of the magnet ($R_{mag_ratio} = R_{mag}/R_o$), the ratio of the height of the coil to the height of the entire volume

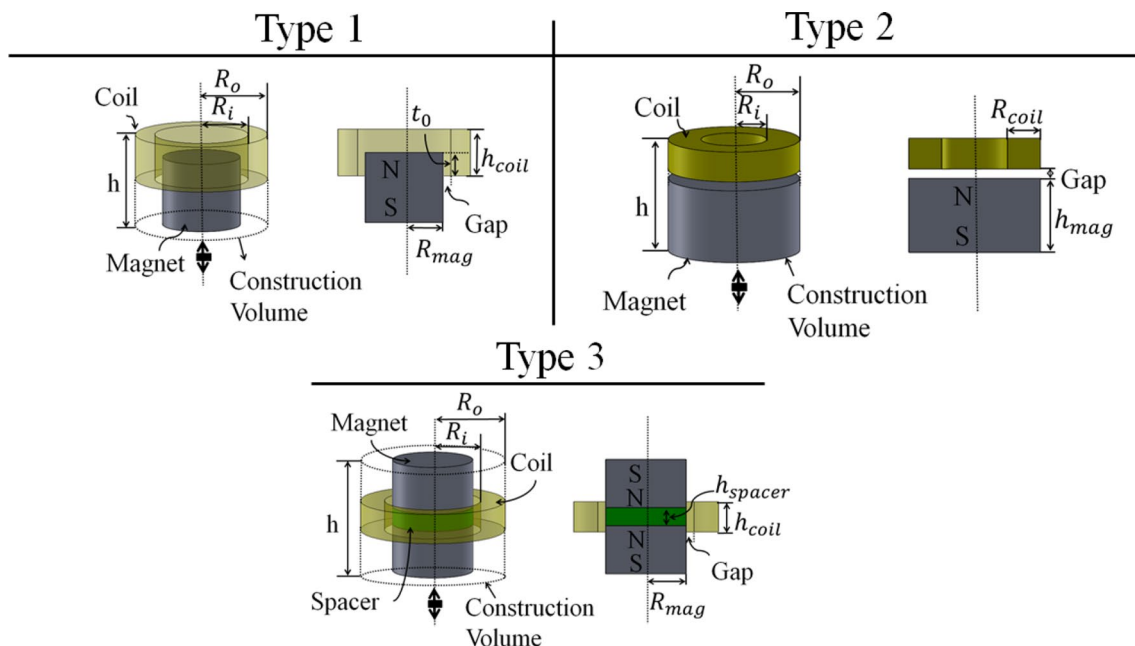


Fig. 3 Geometrical parameters for basic three types of electro-magnetic vibration energy harvester

($h_{coil_ratio} = h_{coil}/h$), and the ratio of the magnet length, that penetrated into the coils ($t_{0_ratio} = t_0/h_{coil}$).

Type 2 is a structure in which a magnet vibrates outside a circular coil. The design variables of Type 2 are the ratio of the radius of the total volume to the radius of the coil ($R_{coil_ratio} = R_{coil}/R_o$) and the ratio of the height of the magnet to the height of the entire volume ($h_{mag_ratio} = h_{mag}/h$).

Type 3 is similar to Type 1 but has two magnets attached to one another with the same polarity facing each other across the spacer, which allows the flow of magnetic fields to be more concentrated. The design variables for optimization of Type 3 are the ratio of the radius of the entire volume to the radius of the magnet ($R_{mag_ratio} = R_{mag}/R_o$), the height the height ratio of the coil to the total volume ($h_{coil_ratio} = h_{coil}/h$), and the ratio of the height of the total volume to the height of the spacer ($spc_ratio = h_{spacer}/h$).

The fixed variables used in this study are shown in Table 2. The total volume was determined as 8 cm³, and the radius R_o and height h of the whole volume were determined by the aspect ratio. The maximum displacement (Z_{lim}) of the magnet and the gap (G) between the magnet and the coil were both set to 0.5 mm. The properties of the magnets were defined using NdFeB N35 and the spacer using steel 1008. In addition, 0.19 mm copper wire was used for the coil, and coil properties were defined using IEC60317 [19].

3.2 Optimization Procedure

The aspect ratio (AR) is defined as the height (h) relative to the diameter ($D = 2R_o$) of the total volume for comparison of the output performance of harvesters with the same volume. The aspect ratio was set from 0.1 to 3.2, and the optimization was performed for six aspect ratios, 0.1, 0.2, 0.4, 0.8, 1.6, and 3.2, considering the shape.

The output voltage and the output power were maximized for the type and aspect ratio of the harvester, respectively, and the optimum design formulation for the output voltage and power are as shown in Eqs. (21) and (22), respectively. x_i is a design variable for each type of harvester:

$$\text{Maximize } V_{rms}, \tag{21}$$

$$\text{Maximize } P_{avg}, \tag{22}$$

$$V_{constraint} = 8 \text{ cm}^3,$$

$$AR = 0.1, 0.2, 0.4, 0.8, 1.6, 3.2,$$

$$0.1 \leq x_i \leq 0.9.$$

To optimize the design of the electromagnetic vibration energy harvester, an approximate optimal design using the orthogonal array and the kriging technique was performed using the commercial program JMP.

3.3 Optimization Result

Figure 4 shows the maximum output voltage and power according to the aspect ratio for the three types of harvesters. Regardless of the aspect ratio, Type 3 had the best performance in terms of output voltage and power, and Type 1 had the smallest output. It can also be seen that there was almost no difference between the result obtained by the kriging metamodel and the calculated value using the numerical integration of the differential equation.

Figure 4a shows the maximum voltage when the aspect ratio is 0.8 in all three shapes, and Fig. 4b shows the

Table 2 Fixed parameters of harvester

Description	Symbol	Value
Construction volume	V_{const}	8 cm ³
Maximum inner displacement	Z_{lim}	0.5 mm
Gap between coil and magnet	G	0.5 mm
Density of magnet	ρ_{mag}	7400 kg/m ³
Density of steel1008	ρ_{steel}	7850 kg/m ³
Coil		
Copper fill factor	k_{co}	0.53
Wire diameter	d_{co}	0.19 mm
Resistance per unit length	R_p	0.603 Ω /m

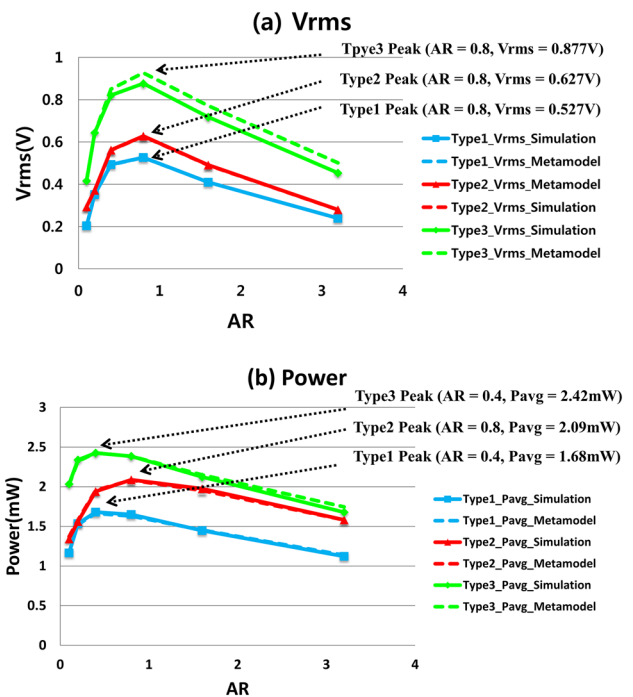


Fig. 4 a Maximum voltage and b maximum power for different aspect ratios

maximum power when the aspect ratio is 0.4 in Type 1 and Type 3 harvesters and 0.8 in Type 2 harvesters.

The optimal values of the design variables for the three types are shown in Fig. 5. If we look at the design variables that maximize the output voltage and power, we can see that all design variables have a nearly constant value regardless of the aspect ratio.

Figure 5a shows the optimal ratio of the design variables of Type 1 harvester. For the output voltage, the optimum ratio is R_{mag_ratio} at 0.6, h_{coil_ratio} at 0.65, and t_0_ratio at 0.5. For the output power, the optimum ratio is R_{mag_ratio} at 0.85, h_{coil_ratio} at 0.3 and t_0_ratio at 0.65.

Figure 5b shows the optimal ratio of the design variables of Type 2 harvester. For the output voltage, R_{coil_ratio} is 0.85, h_{mag_ratio} is 0.5, is an optimum ratio. For the output power, R_{coil_ratio} is 0.5, h_{mag_ratio} is 0.8, is an optimum ratio.

Figure 5c shows the optimal ratio of the design variables of Type 3 harvester. For the output voltage, the optimum ratio is R_{mag_ratio} at 0.6, h_{coil_ratio} at 0.6, and spc_ratio at 0.1. For the output power, the optimum ratio is R_{mag_ratio} at 0.85, h_{coil_ratio} at 0.4, and spc_ratio at 0.15.

Figure 6 gives the optimal shape for the output power when the aspect ratio is 0.2, 0.8 in the Type 1 harvester

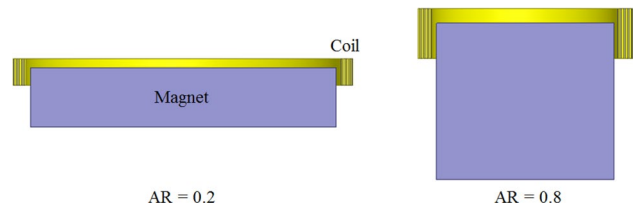


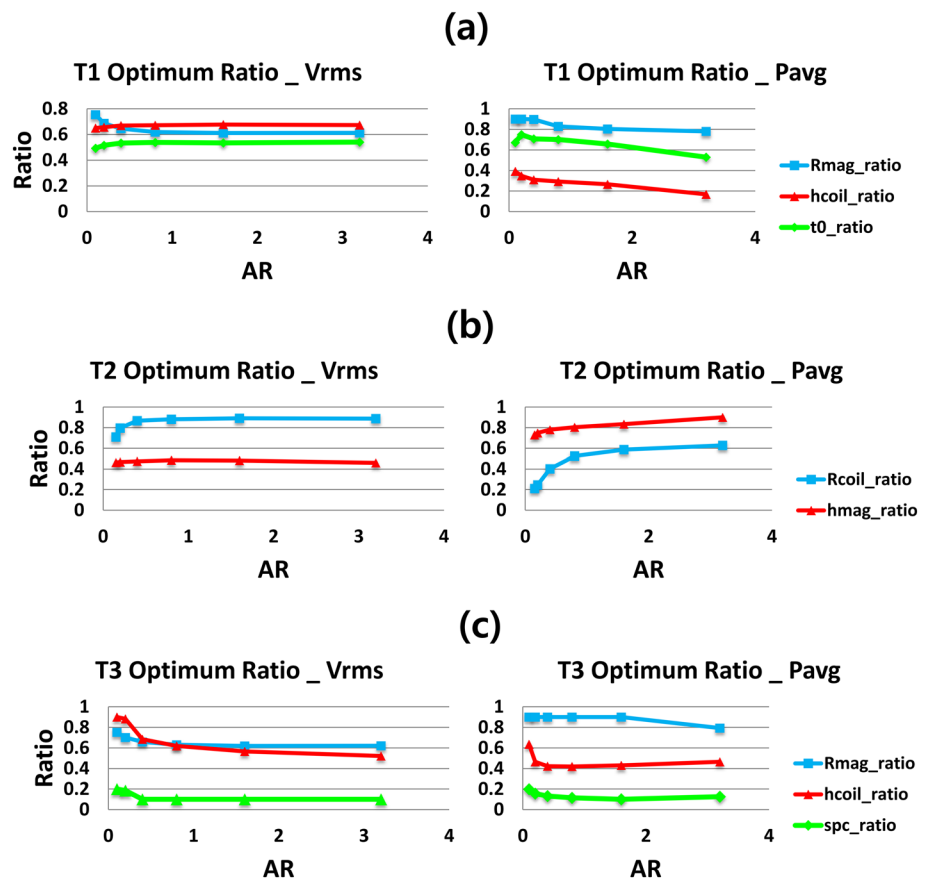
Fig. 6 Optimum design of Type 1 for aspect ratio = 0.2, 0.8

4 Experimental Validation

4.1 Experiment Setup and Experiment Specimens

We verified the simulation results using an experiment that was based on a shaker with an accelerometer, as shown in Fig. 7a. The exciter was set with an exciter controller and vibrated at desired excitation conditions. The exciter controller measured the exciter signal in real time using an accelerometer connected to amplifiers. The magnet and coil were fixed to the zig as shown in Fig. 7b, and the height between the magnet and the coil was accurately set using the height gauge. The coil was connected to a resistor, and the induced voltage at the resistor was measured by an oscilloscope while

Fig. 5 Optimized parameters for output voltage and power of a Type 1, b Type 2 and c Type 3



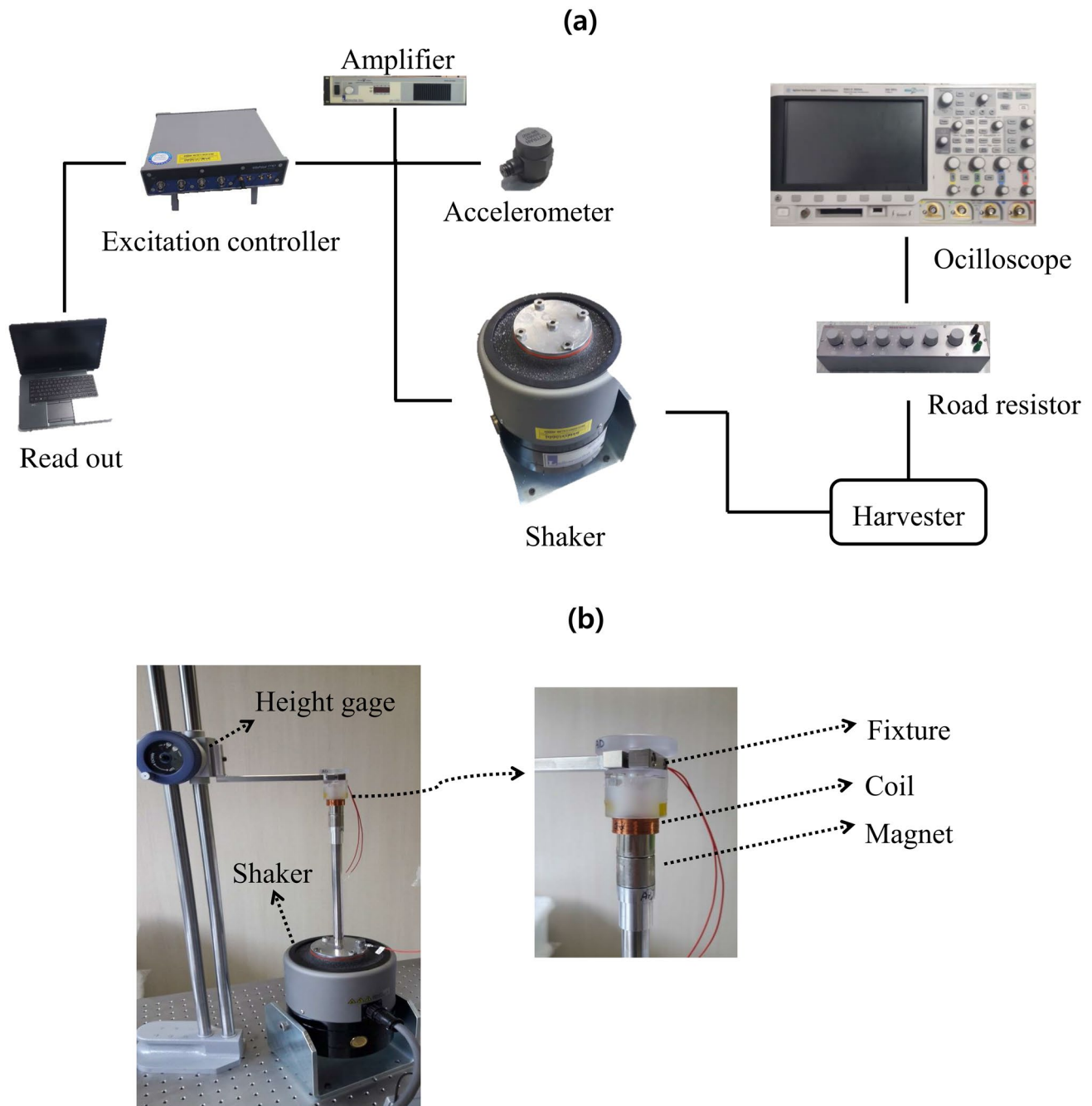


Fig. 7 Equipment used for the **a** set-up and the **b** experiment specimen set on the test device

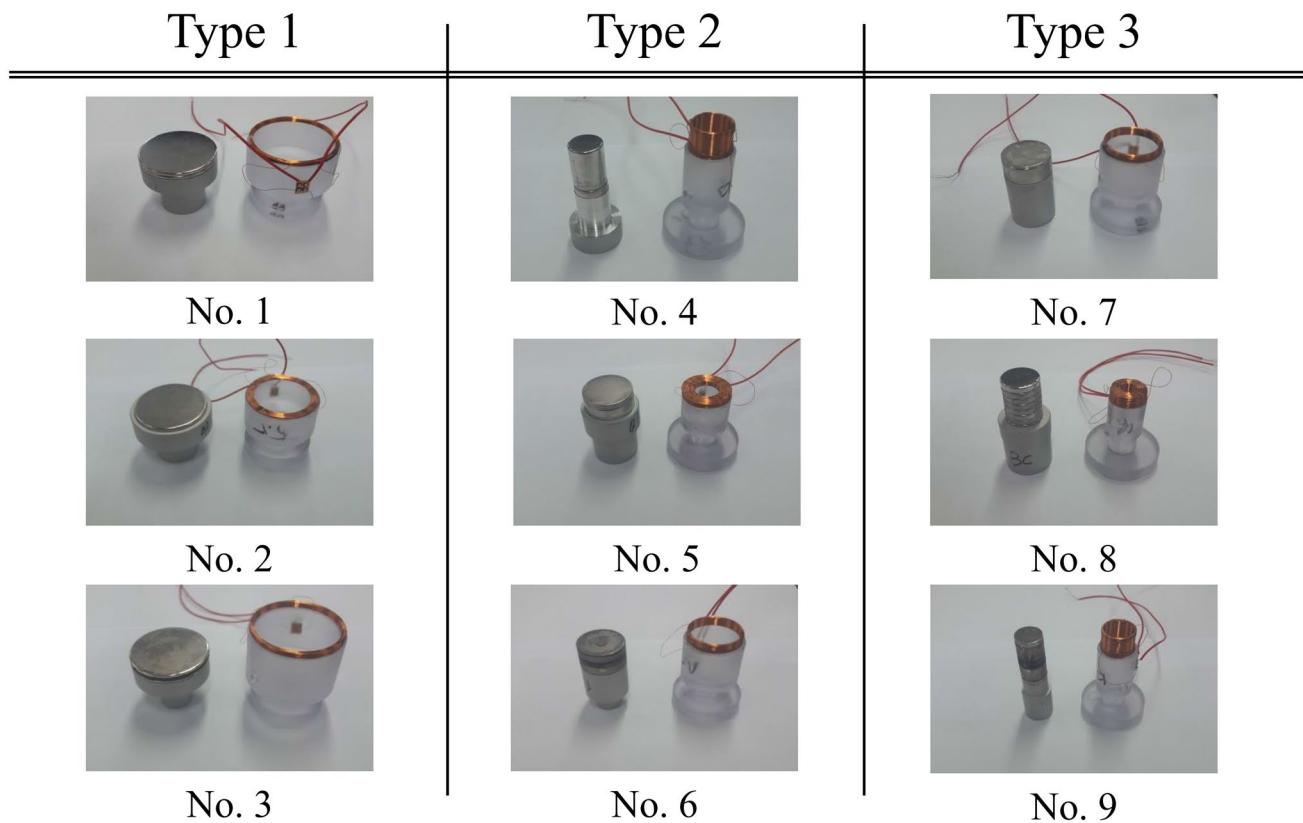
the shaker was vibrated with set vibration conditions. The output power of the harvester was calculated using the measured induced voltage and Eqs. (14) and (15). Furthermore, the transduction factor was calculated by the maximum voltage and excitation speed measured in the experiment. The excitation conditions were the same as the conditions used in Table 1.

The harvester used in the experiment was fabricated with the design parameters shown in Table 3. The aspect

ratio and design parameters of each type were designed to be similar to the optimized design value for the output power based on simulation results. To verify the optimum aspect ratio of each type, the harvester was designed by dividing the harvester range into a small aspect ratio range of 0.1–0.2, an optimum aspect ratio range of 0.4–0.7, and a high aspect ratio range of 1.6–1.7, as shown in Fig. 8.

Table 3 Experiment design parameters

	Type 1			Type 2			Type 3		
No.	1	2	3	4	5	6	7	8	9
AR	0.12	0.43	1.65	0.16	0.65	1.75	0.11	0.43	1.60
R_{mag_ratio}	0.90	0.87	0.82	–	–	–	0.89	0.87	0.81
h_{coil_ratio}	0.40	0.34	0.41	–	–	–	0.60	0.41	0.42
t_0_ratio	0.45	0.70	0.70	–	–	–	–	–	–
R_{coil_ratio}	–	–	–	0.22	0.50	0.58	–	–	–
h_{mag_ratio}	–	–	–	0.78	0.80	0.80	–	–	–
SPC_ratio	–	–	–	–	–	–	0.20	0.18	0.16
Optimal case	–	√	–	–	√	–	–	√	–

**Fig. 8** Design of experiment specimen

4.2 Experiment Result

In the experimental validation, we first verified the transduction factor calculated from the FE analysis. The transduction factor is a key factor in determining the output result of the harvester. From the induced voltage and excitation velocity measured in the experiment, the transduction factor was calculated using Eq. (13). Table 4 show a comparison of the calculation result of the transduction factor between the simulation and the experiment with experiment cases No. 2, No. 5 and No. 8, which had been classified as the optimum aspect ratio based on simulation results. The transduction

Table 4 Comparison of transduction factor

Experiment number	Simulation (V/m/s)	Experiment (V/m/s)	Difference (%)
No. 2	2.7	2.66	1.5
No. 5	4.34	4.13	4.8
No. 8	5.64	5.78	2.4

factors calculated by the FE analysis were very similar to the experimental results, thus verifying the validity of the FE analysis used in this study.

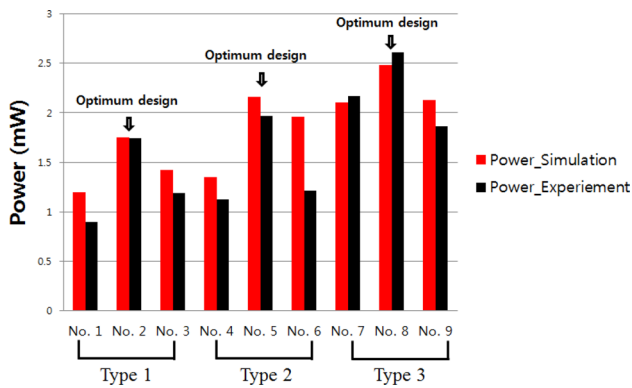


Fig. 9 Comparison of simulation power result and measured power

For verification of the optimum aspect ratio, the experimental results were compared with the simulation results for the output power as shown in Fig. 9. Overall, it is clear that the simulation results were similar to the experimental results. The maximum output power of each type was in the range of 0.4–0.8, which was similar to the simulation result. We also confirmed that the size of the optimized output power was larger in the order of Type 3, Type 2, and Type 1, as in the simulation. However, in the case No. 6 experiment, the error rate was about 60 percent. In other experiments, it was possible to make the design with the combination of two or three magnets, but in the case No. 6 experiment, there was no proper standard among the magnets sold, so seven magnets were combined. Therefore, we judged that there was a large error compared with the other experiments. Nevertheless, we can confirm that the results of the experiment and the simulation generally agreed with each other

5 Conclusions

In this study, was performed and compared the optimum design of three basic types of electromagnetic vibration energy harvester with their aspect ratio. In addition, we presented numerical values optimized for the type and aspect ratio as specific ratios. For accurate and efficient calculation, the output voltage and power were calculated using finite element analysis and differential equations. This study confirmed that the predicted values using an approximate model and the actual calculated values were very similar in all three shapes. We further conducted experiments to verify the simulation results. Through the design optimization results, the output voltage and power for the same volume of all three types of harvester had a maximum at an aspect ratio ranging from 0.4 to 0.8, thus confirming the optimal design values for each aspect ratio. Since all the design parameters were a generalized optimized design as a dimensionless ratio, the

design can be applied to various types of vibration energy harvester without being limited by size in determining and arranging shapes of magnets and coils.

Acknowledgements This study is a research carried out with the support of the Korea Institute of Machinery and Materials in 2016.

References

- Spreemann, D., & Manoli, Y. (2012). *Electromagnetic vibration energy harvesting devices: Architectures, designs, modeling and optimization, advanced microelectronics* (Vol. 35). New York: Springer.
- Beeby, S. P., Torah, R. N., Tudor, M. J., et al. (2007). A micro electromagnetic generator for vibration energy harvesting. *Journal of Micromechanics and Microengineering*, 17, 1257–1265.
- And, Williams C., & Yates, R. (1996). Analysis of a micro-electric generator for microsystems. *Sensors and Actuators, A: Physical*, 52, 8–11.
- Arnold, D. P. (2007). Review of microscale magnetic power generation. *IEEE Transactions on Magnetics*, 43(11), 3940–3951.
- Kim, J. E., Kim, H. J., Yoon, H. S., & Kim, Y. Y. (2015). An energy conversion model for cantilevered piezoelectric vibration energy harvesters using only measurable parameters. *International Journal of Precision Engineering and Manufacturing-Green Technology*, 2(1), 51–57.
- Jin, J. W., Kim, J. H., & Kang, K. W. (2015). Development of durability test procedure of vibration based energy harvester in railway vehicle. *International Journal of Precision Engineering and Manufacturing-Green Technology*, 2(4), 353–358.
- Park, H. C., & Kim, J. H. (2016). Electromagnetic induction energy harvester for high speed railroad applications. *International Journal of Precision Engineering and Manufacturing-Green Technology*, 3(1), 41–48.
- Park, H. C. (2017). Vibration electromagnetic induction energy harvester on wheel surface of mobile sources. *International Journal of Precision Engineering and Manufacturing-Green Technology*, 4(1), 59–66.
- Kim, J. H., Shin, Y. J., Chun, Y. D., & Kim, J. H. (2018). Design of 100 W regenerative vehicle suspension to harvest energy from road surfaces. *International Journal of Precision Engineering and Manufacturing-Green Technology*, 19(7), 1089–1096.
- Spreemann, D., Hoffmann, D., Folkmer, B., & Manoli, Y. (2008). Numerical optimization approach for resonant electromagnetic vibration transducer designed for random vibration. *Journal of Micromechanics and Microengineering*, 18(10), 104001.
- Spreemann, D., Folkmer, B., & Manoli, Y. (2008). Comparative study of electromagnetic coupling architectures for vibration energy harvesting devices. *Proceedings of the Power MEMS, 2008*, 257–260.
- Cepnik, C., & Wallrabe, U. (2010). Practical and theoretical limits of the output power of electromagnetic energy harvesters at miniaturization. *Proceedings of the Power MEMS, 2010*, 69–72.
- Cepnik, C., Yeatman, E. M., & Wallrabe, U. (2012). Effects of nonconstant coupling through nonlinear magnetics in electromagnetic vibration energy harvesters. *Journal of Intelligent Material Systems and Structures*, 23, 1533–1541.
- Kim, S. C., Kim, Y. C., Seo, J. H., & Lee, H. M. (2017). Design optimization of electromagnetic vibration energy harvesters considering aspect ratio. *The Korean Society for Noise and Vibration Engineering*, 27(3), 360–371.
- Stephen, N. G. (2005). On energy harvesting from ambient vibration. *Journal of Sound and Vibration*, 293(1–2), 409–425.

16. Cepnik, C., Radler, O., Rosenbaum, S., et al. (2011). Effective optimization of electromagnetic energy harvesters through direct computation of the electromagnetic coupling. *Sensors and Actuators, A: Physical*, 167(2), 416–421.
17. Lee, H. M., Kim, Y. C., Lim, J. W., et al. (2014). Design optimization process for electromagnetic vibration energy harvesters using finite element analysis. *Transactions of the Korean Society for Noise and Vibration Engineering*, 24(10), 809–816.
18. Owen, A. (1992). Orthogonal arrays for computer experiments, integration, and visualization. *Statistica Sinica*, 2(2), 439–452.
19. IEC 60317. (2013). Specifications for particular types of winding wires.

Publisher's Note Springer Nature remains neutral with regard to jurisdictional claims in published maps and institutional affiliations.



Seok-Chan Kim is a researcher at Korea Institute of Machinery and Materials (KIMM). He received his B.S. and M.S. in mechatronics engineering from Chungnam National University.



Jin-Gyun Kim is an assistant professor at Kyung Hee University. He received his Ph.D. in Ocean Systems Engineering from Korea Advanced Institute of Science and Technology (KAIST).



Young-Cheol Kim is a principal researcher at Korea Institute of Machinery and Materials (KIMM). He received his Ph.D. in mechanical engineering from Korea Advanced Institute of Science and Technology (KAIST).



Seok-Jo Yang is a professor at Chungnam National University. He received his Ph.D. in Biomedical Engineering from Iowa State University.



Hanmin Lee is a principal researcher at Korea Institute of Machinery and Materials (KIMM). He received his B.S., M.S. and Ph.D. in mechanical engineering from Korea Advanced Institute of Science and Technology (KAIST).